CO2-plant effects do not account for the gap between dryness indices and projected dryness impacts in CMIP5 or CMIP6

Jacob Scheff[1], Justin S Mankin[2], Sloan Coats[3], and Haibo Liu[4]

[1]UNC Charlotte
[2]Dartmouth College
[3]University of Hawaii
[4]columbia university

November 22, 2022

Abstract

Recent studies have found that terrestrial dryness indices like the Palmer Drought Severity Index, Standardized Precipitation Evapotranspiration Index, and Aridity Index calculated from climate model projections are mostly negative, implying a drier land surface with future warming. Yet, the same models' prognostic runoff and bulk soil moisture projections instead feature regional signals of varying sign, suggesting that the dryness indices could overstate climate change's direct impacts. Observed trends also show this "index-impact gap." Most studies have attributed this gap to the indices' omission of CO2-driven stomatal closure. However, here we show that the index-impact gap is still wide even in model experiments that switch off CO2 effects on plants. In these simulations, mean PDSI, Aridity Index, and SPEI still decline broadly with warming, while mean runoff and bulk soil moisture still respond more equivocally. This implies that CO2-plant effects are not the dominant or sole reason for the index-impact gap.

CO_2-plant effects do not account for the gap between dryness indices and projected dryness impacts in CMIP5 or CMIP6

Jacob Scheff[1], Justin S. Mankin[2,4], Sloan Coats[3], and Haibo Liu[4]

[1]Dept. of Geography and Earth Sciences, University of North Carolina Charlotte
[2]Dept. of Geography and Dept. of Earth Sciences, Dartmouth College
[3]Dept. of Earth Sciences, University of Hawaii
[4]Lamont-Doherty Earth Observatory of Columbia University

Key Points:

- Climate models project much more widespread drying using the Aridity Index, PDSI, or SPEI than using runoff or deep soil moisture
- This gap persists even in simulations that turn off CO_2 effects on plant physiology, which were thought to be its main cause
- Thus, it must have a more basic cause than CO_2 effects on plants

Corresponding author: Jacob Scheff, `jscheff@uncc.edu`

Abstract

Recent studies have found that terrestrial dryness indices like the Palmer Drought Severity Index, Standardized Precipitation Evapotranspiration Index, and Aridity Index calculated from climate model projections are mostly negative, implying a drier land surface with future warming. Yet, the same models' prognostic runoff and bulk soil moisture projections instead feature regional signals of varying sign, suggesting that the dryness indices could overstate climate change's direct impacts. Observed trends also show this "index-impact gap."

Most studies have attributed this gap to the indices' omission of CO_2-driven stomatal closure. However, here we show that the index-impact gap is still wide even in model experiments that switch off CO_2 effects on plants. In these simulations, mean PDSI, Aridity Index, and SPEI still decline broadly with warming, while mean runoff and bulk soil moisture still respond more equivocally. This implies that CO_2-plant effects are not the dominant or sole reason for the index-impact gap.

Plain Language Summary

Climate scientists have traditionally measured "drought" and "aridity" using simple formulas based on precipitation and temperature. When these formulas are applied to computer model projections of global warming, they forecast widespread increases in dryness, due to rising temperatures. Yet, these same models also directly simulate river flow and soil moisture – and do not forecast similarly widespread declines in either. Thus, it is unclear whether the drought and aridity formulas are relevant under climate change.

Most existing studies that examine this discrepancy blame the effect of increasing CO_2 on the microscopic pores, called stomata, that help plants conserve water. However, other studies point to more fundamental differences between the drought formulas and the direct simulations. In the present study, we show that the discrepancy persists even in special global warming simulations in which CO_2 effects on stomata are eliminated. This suggests that CO_2 effects on plants are far from the only cause of the discrepancy, and that more work needs to be done to understand it.

1 Introduction

Drought is a surface water shortage, usually driven by below-normal precipitation (P), that negatively impacts water resource production (i.e., stream runoff and groundwater recharge) and/or photosynthesis, with societal consequences (e.g., Wilhite & Glantz, 1985; AMS Council, 2013). *Aridity* is a permanent, climatological lack of enough P to support plentiful regional water resources or vegetation (Budyko & Miller, 1974; Middleton & Thomas, 1997), which plays a key role in human settlement patterns (e.g., Seager et al., 2018).

However, because water resource production and photosynthesis are strongly constrained by the evaporative environment as well as P, the most effective methods for quantifying aridity and drought from climate data require both P and potential evaporation E_0. E_0 integrates radiation, temperature, humidity, and wind speed to quantify the rate at which the atmosphere is capable of evaporating surface water (e.g., Hartmann, 2016). The aridity index or AI (Transeau, 1905; Middleton & Thomas, 1997) is the ratio P/E_0 of annual climatological means. The Standardized Precipitation-Evapotranspiration Index or SPEI (Vicente-Serrano et al., 2010) is the difference $P-E_0$ smoothed to a user-defined timescale and transformed to a normal distribution. The Palmer Drought Severity Index or PDSI (Palmer, 1965) is a bucket model of soil moisture forced by monthly P and E_0. Lower AI and more negative PDSI and SPEI values indicate drier conditions, with reduced water resources and vegetation. These indices are widely used and understood.

According to the standard Penman-Monteith equation (Monteith, 1981; R. G. Allen et al., 1998), E_0 substantially increases with greenhouse warming, mainly due to its dependence on temperature (Scheff & Frierson, 2014). Since projected changes in land P with warming are much less robust (e.g., IPCC, 2013; Greve & Seneviratne, 2015), global-scale climate model studies of AI (Feng & Fu, 2013; Fu & Feng, 2014; Scheff & Frierson, 2015; Huang et al., 2015; Fu et al., 2016; Zarch et al., 2017; Park et al., 2018; Wang et al., 2020), PDSI (Dai, 2013; B. I. Cook et al., 2014; Zhao & Dai, 2015, 2016; Lehner et al., 2017), and SPEI (B. I. Cook et al., 2014; Touma et al., 2015; Naumann et al., 2018) almost always obtain widespread drying in warming scenarios. The same models also project widespread declines in near-surface soil moisture $\mathrm{SM_s}$ (Dai, 2013; IPCC, 2013; Berg et al., 2017) and relative humidity RH (IPCC, 2013; Byrne & O'Gorman, 2016), which are used to argue for the physical relevance of the AI- or PDSI-based drying (e.g., Sherwood & Fu, 2014; Dai et al., 2018).

Yet, as argued above, the core purpose of AI, PDSI, and SPEI, and the main use of $\mathrm{SM_s}$, is to indicate negative impacts to water-resource production and/or photosynthesis (Roderick et al., 2015; Greve et al., 2017; Scheff et al., 2017; Scheff, 2018). And, the same models that project widespread global declines in AI, PDSI, SPEI, $\mathrm{SM_s}$, and RH with warming project much more equivocal, two-sided changes in water-resource generation (IPCC, 2013; Roderick et al., 2015; Zhao & Dai, 2015, 2016; Swann et al., 2016; Milly & Dunne, 2016, 2017; Greve et al., 2017; Scheff et al., 2017) and deep-layer soil moisture $\mathrm{SM_d}$ (Berg et al., 2017; Berg & Sheffield, 2018; Greve et al., 2019). Furthermore, these models project ubiquitous *increases* in photosynthesis (Greve et al., 2017, 2019; Scheff et al., 2017; Mankin et al., 2018) and leaf coverage (Mankin et al., 2019), a.k.a. "greening." Thus, it is not clear if the AI, PDSI, and SPEI projections are actually relevant for warming impacts on water availability, nor (likewise) if the models' prognostic runoff, $\mathrm{SM_d}$, and/or vegetation projections are reliable. Scheff (2018) and Scheff et al. (2017) show that this "index-impact gap" is also clear in global *observations* during $\mathrm{CO_2}$-driven climate changes (both recent and geologic), lending it additional credence. However, it is much less pronounced in certain regions, such as the American Southwest (B. I. Cook et al., 2015; Ault et al., 2016), particularly for $\mathrm{SM_d}$.

What is the reason for this discrepancy? Most of the above studies argue that AI, PDSI and SPEI do not resemble projected climate change impacts in many places mainly because they do not account for the beneficial effect of elevated $\mathrm{CO_2}$ on plant water requirements, which tends to reduce evapotranspiration (ET) and increase photosynthesis (Roderick et al., 2015; Swann et al., 2016; Greve et al., 2017, 2019; Milly & Dunne, 2017; Scheff et al., 2017). Yang et al. (2019, 2020) modify the standard Penman-Monteith equation to include this stomatal effect and find that the resulting AI and PDSI come much closer to the models' hydrologic projections, and Lemordant et al. (2018) show that $\mathrm{CO_2}$-plant effects dramatically alter key model hydrologic outputs. Certainly, the bulk of simulated greening would not occur without these simulated $\mathrm{CO_2}$ effects (Arora et al., 2013; Shao et al., 2013).

However, many other proposed causes of the index-impact gap, especially with regard to hydrologic impacts (i.e., water resources and $\mathrm{SM_d}$), are unrelated to $\mathrm{CO_2}$-plant effects. Zhao and Dai (2015), Dai et al. (2018), and Mankin et al. (2018) argue that the gap occurs partly because the increase in instantaneous P *rate* in a warming world drives greater runoff production for the same long-term total P. Observed and projected shifts in P towards the hydrological wet season (e.g., Chou et al., 2013; R. J. Allen & Anderson, 2018) would have the same effect, and Berg et al. (2017) argue that the gap between $\mathrm{SM_d}$ and $\mathrm{SM_s}$ also stems from rectification of the seasonal cycle. Massmann et al. (2019) show that warming itself may reduce ET by closing stomata (Novick et al., 2016), apart from $\mathrm{CO_2}$. Further, Mankin et al. (2019) find that in much of the mid-latitudes, the projected increase in leaf area due to CO_2 and warming cancels any plant water savings from CO_2-induced stomatal closure, so that the net hydrologic impact of CO_2-plant effects is often negative, not positive. Lehner et al. (2019) argue that prognostic runoff responses to climate change are biased positive, because model runoff seems to be too sensitive to P, and not sensitive enough to warming. Finally, Milly and Dunne (2016) and Vicente-Serrano et al. (2019) argue that Penman-Monteith E_0 (and thus AI, PDSI and SPEI) is not always relevant to real watersheds under climate change, regardless of CO_2 effects.

Thus, it is not at all clear that CO_2-plant effects are the main reason why simulated and observed mean hydrologic impacts of climate change are not as negative as AI, PDSI, or SPEI in many regions. Indeed, Milly and Dunne (2016) found that in one model, the gap between AI and runoff responses persisted even when those effects were switched off, at least in the global average. Here, we extend that comparison to many more models, variables, and regions, showing that even when CO_2-plant effects are suppressed, mean AI, PDSI, and SPEI (index) projections are much more widely negative than mean runoff, SM_d, or vegetation (impact) projections.

2 Data and methods

We examine monthly output equatorward of 55° from 11 climate models in the Coupled Model Intercomparison Project phase 6 (CMIP6; Eyring et al., 2016), listed in Table S1 in the Supporting Information. We compare the results of two experiments that strongly warm the planet by increasing CO_2 1% per year for 140 years (or more). In experiment "1pctCO2", both the vegetation and radiation schemes "see" the increasing CO_2, as in the experiments discussed in Section 1. Experiment "1pctCO2-rad" (Jones et al., 2016) is identical to 1pctCO2 except that the vegetation schemes instead "see" a constant 280 ppm of CO_2, so any index-impact gap in 1pctCO2-rad must occur for a reason *other* than simulated CO_2-plant effects.

For each model, the climatological annual-mean responses of P, E_0, AI, PDSI, SPEI, RH, SM_s, SM_d, water resource generation (i.e., total runoff Q), runoff ratio Q/P, photosynthesis, leaf area index LAI, and evaporative fraction EF are quantified using the difference between years 111-140 and years 1-30 of the "r1i1p1" run, except where noted in Table S1. Monthly E_0 is computed using the standard Penman-Monteith equation (R. G. Allen et al., 1998) and AI for each 30-year period is the ratio of 30-year-mean P to 30-year-mean E_0, all as in Scheff et al. (2017). PDSI and 12-month SPEI are computed from monthly P and E_0 as in B. I. Cook et al. (2014) using years 1-30 as the reference period; SPEI is set to -2.33 (100-year drought) when $P-E_0$ is less than the origin of the reference distribution (S. Vicente-Serrano, pers. comm.). As in Scheff et al. (2017), monthly RH is defined as monthly-mean vapor pressure divided by saturation vapor pressure at monthly-mean temperature, for consistency with the E_0 calculation.

SM_s uses the "mrsos" output (mm of water in the top 10 cm of the soil), and SM_d is derived by summing the "mrlsl" output (mm of water in each soil layer) to a depth of 2 m, using a fraction of the bottom layer if necessary. They are each converted to volumetric water content (m^3/m^3), by dividing by 100 mm and 2000 mm respectively. Q is calculated as P minus ET rather than using model runoff output, to emphasize total water-resource generation and avoid inconsistencies in how models defined runoff. Q/P, which AI predicts in the present climate (Gentine et al., 2012), is the ratio of 30-year means. Photosynthesis is quantified using gross primary productivity (GPP), which is the flux of carbon through the stomata (Bonan, 2015) and thus the most water-linked metric. EF, a close cousin of the Bowen ratio, is the fraction of the 30-year-mean total turbulent heat flux (LH+SH) made up by the latent heat flux LH; decreases in EF represent drought impacts to the atmosphere.

For each variable, the responses are nearest-neighbor interpolated to a common 3° grid, and multi-model statistics are taken. For SM_d, only nine models are available (Table S1); restricting the remainder of the study to only those models does not substantially change the results below. We also conduct a similar analysis on the CMIP5 (Taylor et al., 2012) 1pctCO2 vs. "esmFdbk1" experiments, with details and results in the Supporting Information.

3 Results

Fig. 1 maps the median responses to the "standard" 1pctCO2 experiment, in which both climate and vegetation respond to the CO_2 increase. The index-impact gap common to the coupled models is apparent: RH, AI, SPEI, PDSI, and SM_s (Figs. 1a-e) robustly and widely decline, but EF, SM_d, Q/P, and Q respond much more heterogeneously (i.e., more like P; Figs. 1f-j), and LAI and GPP robustly and near-ubiquitously increase (Figs. 1k-l.) However, EF still resembles PDSI in some places, facially suggesting that PDSI could be relevant for atmospheric impacts (Dai et al., 2018) despite its dissimilarity to water-resource and ecological impacts. Fig. S1 in the Supporting Information reproduces Fig. 1 but using standardized changes; results are similar, except that Q and Q/P responses become much weaker than the other metrics, reinforcing the sense of a gap.

Fig. 2 maps the responses to the 1pctCO2-rad experiment, in which climate responds to the CO_2 increase, but vegetation does not. Despite the lack of any CO_2-plant effects, the index-impact gap is still wide, especially for hydrologic impacts: RH, AI, SPEI, PDSI, and SM_s (Figs. 2a-e) again show widespread robust declines, but the responses of Q/P (Fig. 2h) and especially Q (Fig. 2j) are again much more two-sided. In particular, the Americas are dominated by AI, SPEI, and PDSI "drying", yet have less consistent decreases in Q/P, and regional decreases and increases in Q. In Africa and Australia, Q and Q/P increases are actually more extensive than decreases, despite strongly drying AI, PDSI and SPEI. However, in general, the gap is not quite as large as in Fig. 1, both because RH, AI, SPEI, and PDSI dry slightly less, and because Q and Q/P dry slightly more, consistent with Swann et al. (2016). Thus, CO_2 effects still appear to cause some of the gap, by reducing ET and thus increasing both E_0 and Q in Fig. 1 relative to Fig. 2 (Berg et al., 2016; Brutsaert & Parlange, 1998).

SM_d (Fig. 2g) declines more robustly than Q, but not always as robustly as AI or SPEI, especially in Eurasia, North America and Australia. The declines are still weaker and less consistent than those in SM_s (Fig. 2e). Interestingly, EF (Fig. 2f) responds much more like P (Fig. 2i) than like the indices, SM_s, or even SM_d, implying that the relative consistency of EF with PDSI in Fig. 1 may just be a fortuitous effect of CO_2 reducing ET. Finally, as expected, LAI and GPP (Figs. 2k-l) lose their large, near-ubiquitous increases, but still change little (or even increase) in many regions where AI, SPEI and PDSI strongly decline, particularly in the mid-latitudes and Australia. Fig. S2 reproduces Fig. 2 using standardized changes; again the main difference is relative weakening of the Q and Q/P responses.

Fig. 3 distills Figs. 1 and 2 by plotting each panel as a single point in area-with-robust-drying vs. area-with-robust-wetting space, color-coded by type of metric (where "robust" means stippled on Fig. 1 or 2; that is, $\geq 75\%$ intermodel agreement). It is immediately apparent that while the gap between the index (AI, PDSI, SPEI) and hydrologic impact (Q, Q/P) projections is larger with CO_2-plant effects on (left), it is still large even with CO_2-plant effects turned off (right). In the latter case, for PDSI, more than four times as much land area has robust drying as robust wetting, yet the areas of robust Q increase and robust Q decrease are equal (Fig. 3, right), complicating the interpretation of PDSI as a water-resource proxy under climate change (e.g., E. R. Cook et al., 2009). For AI, more than 10 times as much land area has robust drying as robust

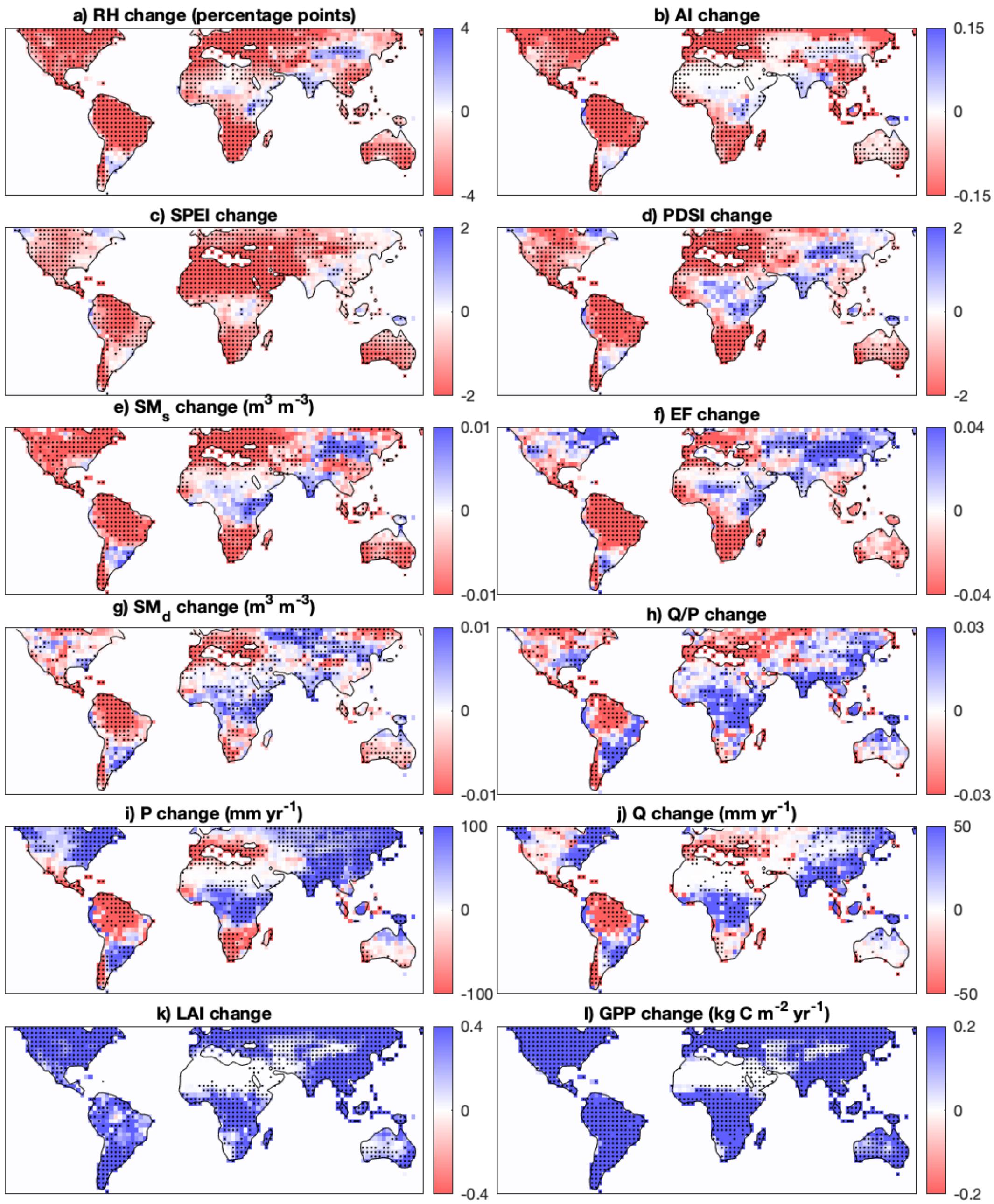

Figure 1. Multi-model median differences between years 111-140 vs. 1-30 of the 1pctCO2 CMIP6 experiment, in which vegetation responds to the CO_2 increase. Black dots show where at least 75% of the models agree on the sign of the change (i.e., where the change is robust.) Variables without units are dimensionless.

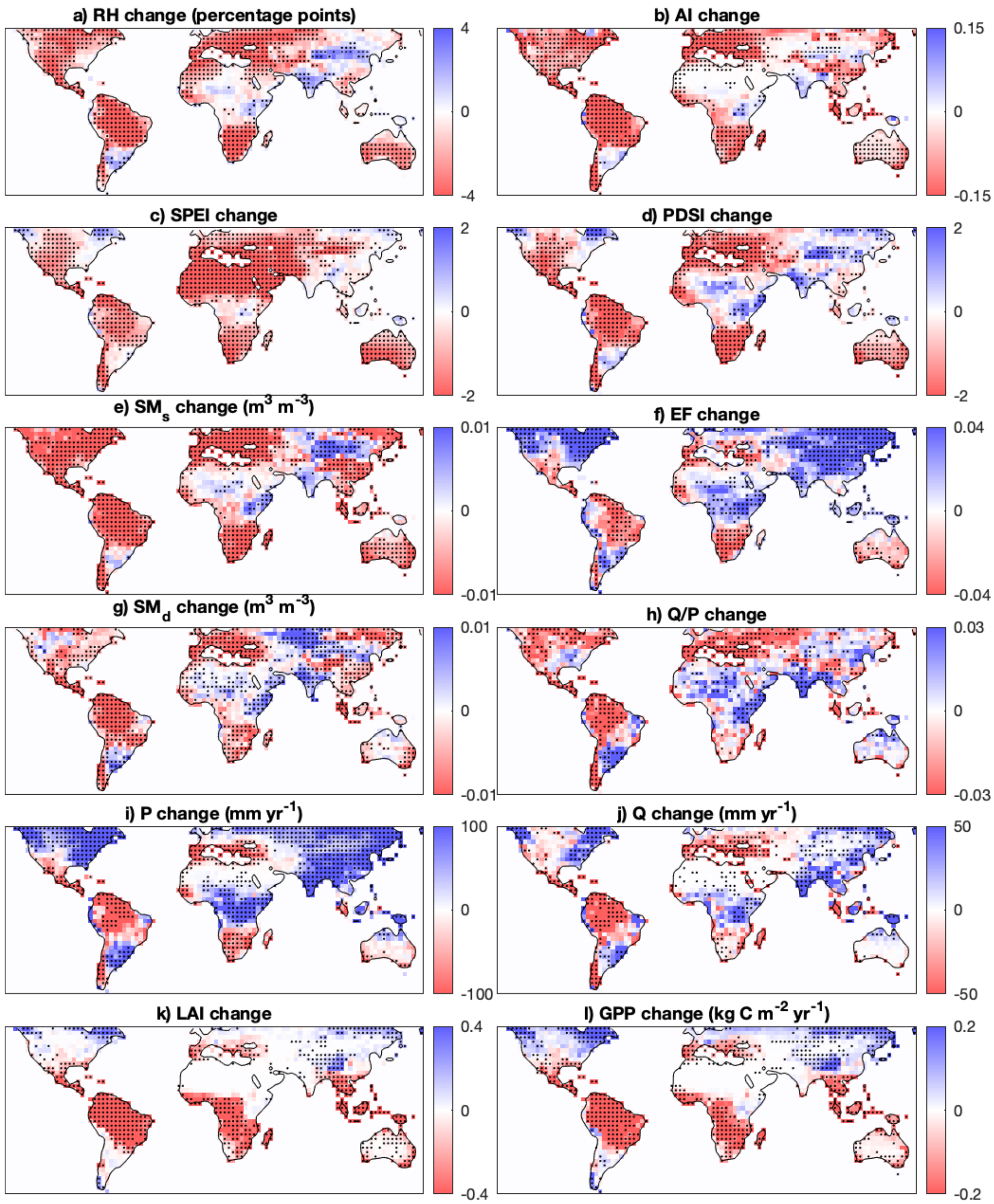

Figure 2. As Fig. 1, but for the 1pctCO2-rad experiment, in which vegetation does not "see" the CO_2 increase.

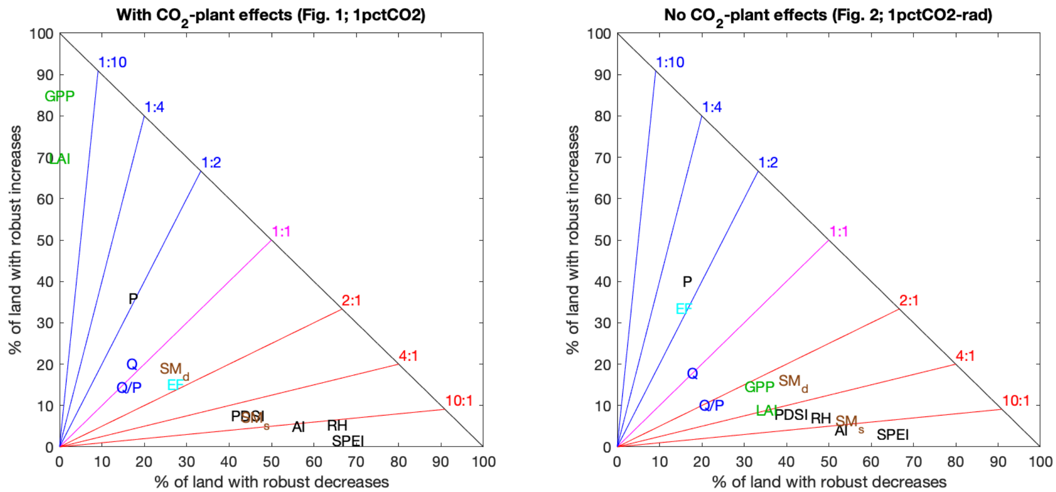

Figure 3. Percent of land area with multi-model robustly projected (i.e., stippled) decreases (x-axis) and increases (y-axis) in each variable on Fig. 1 (left; vegetation responds to CO_2) and Fig. 2 (right; vegetation does not respond to CO_2). Climate variables and indices are in black, vegetation impacts in green, water-resource impacts in dark blue, soil moisture impacts in brown, and atmospheric impacts in light blue. Colored lines mark ratios of robust-decrease area to robust-increase area.

wetting, yet the area of robust Q/P decrease is only twice the area of robust Q/P increase, despite the theoretical basis for AI as the primary driver of Q/P variation in the present climate (Budyko & Miller, 1974).

For SM_d and (especially) GPP and LAI, the gap from AI, PDSI, and SPEI responses without CO_2-plant effects (right) is much smaller than with CO_2-plant effects (left), mainly because the massive GPP and LAI increases are much reduced. However, the gap is still noticeable: similar to Q/P, robust GPP and SM_d decreases are only about 2-3 times more widespread than respective increases, even though robust PDSI, AI and SPEI decreases are over 4, 10, and 20 times more widespread than respective increases. LAI more strongly tends to decrease, similar to PDSI, but still not as much as AI, SM_s or SPEI. Thus, the indices still do not seem to be particularly reliable proxies for projected vegetation-related impacts, even in a world where CO_2 does not affect vegetation. As discussed above in the context of Fig. 1, this is particularly so in parts of the midlatitudes, where growing-season lengthening is an important driver of vegetation increases (e.g., Mankin et al., 2018, 2019). Also, EF is even farther from the indices when CO_2-plant effects are off (right) than on (left), confirming that any apparent relevance of the indices for EF in Fig. 1 is just a fortuitous consequence of CO_2 effects on transpiration.

We quantify several of the index-impact gaps in greater detail by mapping disagreement between the impact variables (Q, Q/P, SM_d, GPP) and the indices and similar variables (AI, PDSI, SPEI, SM_s) across the multi-model ensemble (Fig. 4). Specifically, we map the percentage of models that obtain increases in impact variables despite decreases in index-type variables (minus the percentage that do the opposite, which is much smaller). With CO_2-plant effects on (left column), a large proportion of the models simulate hydrologic and vegetation increases despite declining indices, as expected (though there are also regional exceptions). With CO_2-plant effects turned off (right column), this proportion persists, albeit slightly diminished. Again, the gaps between Q and Q/P and the indices (Fig. 4a-f) and between SM_d and SM_s (Fig. 4g-h) are particularly persistent. (Some very dry regions do have the opposite sign gap, but $Q \approx 0$ in such places.)

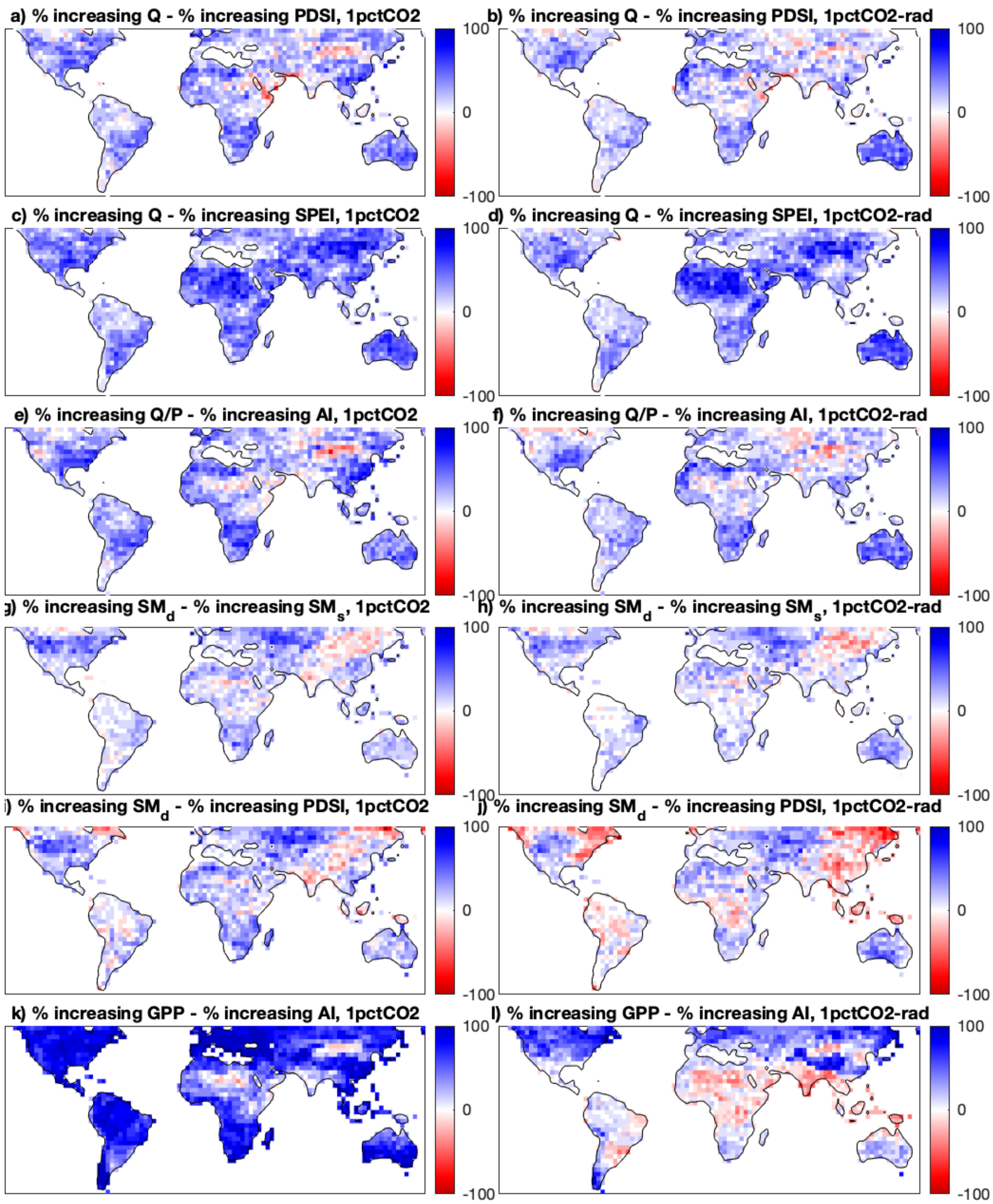

Figure 4. Percent of models with increasing A minus percent of models with increasing B (equivalently, percent of models with increasing A and declining B minus percent of models with increasing B and declining A), for selected pairs of variables A and B. Left: 1pctCO2 (vegetation sees CO_2). Right: 1pctCO2-rad (vegetation does not see CO_2). In panels g through j, both variables use only the 9 models that had SM_d for both experiments (Table S1).

In contrast, the prevalence of SM_d increases despite PDSI declines (Fig. 4i) is more noticeably reduced once CO_2 effects are turned off (Fig. 4j), while regions with the opposite sign gap are expanded. This relative agreement makes sense, since PDSI is a fundamentally a model of SM_d. Finally, the very large proportion of models that increase GPP despite index declines (e.g., Fig. 4k) largely vanishes or reverses in the tropics when CO_2 effects are turned off, but still noticeably persists in the mid-latitudes (Fig. 4l); results are similar for LAI. This again suggests that growing-season lengthening, in addition to CO_2, is a key driver of the gap between index and vegetation responses in the midlatitudes.

Figs. S3-S6 reproduce Figs. 1-4 but using nine CMIP5 models, for cleaner comparison with the literature cited in the Introduction. The results are very similar, though the index-impact gaps (both with and without CO_2) tend to be even wider in CMIP5 than in CMIP6. Whether this is due to model improvement going from CMIP5 to CMIP6, or just different model selection (Table S1 vs. S2), is unknown. The lack of index-impact gaps in CMIP5 in parts of the American Southwest (B. I. Cook et al., 2015; Ault et al., 2016) is also apparent on Fig. S6.

4 Discussion

In short, Figs. 1-4 and S3-S6 show that while some simulated index-impact gaps can be driven by CO_2-plant effects (e.g. low-latitude greening despite index declines, or PDSI declining more than SM_d), most of the others (e.g. Q, Q/P and mid-latitude vegetation increasing despite index declines, and SM_d declining less than SM_s) persist without any CO_2-plant effects. Thus, contrary to studies like Swann et al. (2016), Milly and Dunne (2017), Scheff et al. (2017), and Greve et al. (2017), but in agreement with Mankin et al. (2019) and Greve et al. (2019), we find that CO_2-plant effects are *not* the sole or dominant reason that impact simulations disagree with common climatic dryness indices under global warming. Instead, other mechanisms must be in play to explain the index-impact gaps.

What could those other, non-CO_2 factors be? The easiest explanations are that the indices are just simple formulas, and should not be expected to reflect complex climate change impacts in the first place (e.g., Milly & Dunne, 2016; Greve et al., 2019) - and/or that mean changes in runoff and vegetation production are not actually what the indices are built to measure. However, the indices all have long histories of successful use in the present climate as hydrological and ecological impact proxies, continue to be frequently used to quantify climate change's broad dryness effects (e.g., Lehner et al., 2017; Naumann et al., 2018; Wang et al., 2020), rest on solid theoretical foundations (Penman-Monteith E_0, the Budyko curve, soil moisture modeling, the complementary principle), and do in fact agree with the impact projections in some places (Figs. 4 and S6; B. I. Cook et al., 2015; Ault et al., 2016). Where there are disagreements, they are mostly in one direction (indices drier than simulated impacts; Fig. 4) even with CO_2 effects turned off. Thus, it is important to understand where the differences come from, so as to better assess the relevance and applicability of both types of projections.

For water-resource (Q and Q/P) responses, there is no shortage of potential non-CO_2 mechanisms by which they could skew more positive than index responses, as detailed in Section 1. Again, these include direct closure of leaf stomata by high temperatures and vapor-pressure deficits (Novick et al., 2016; Massmann et al., 2019), concentration of P into fewer, heavier events (e.g., Mankin et al., 2018; Dai et al., 2018), and concentration of P into the hydrological wet season (e.g., Chou et al., 2013), all of which are accounted for in the models but not in the indices. Biases in model Q and Q/P sensitivity to P and temperature (Lehner et al., 2019) could also be important. More broadly, some of the gap between Q and PDSI responses could also simply be that PDSI is a soil-moisture model, despite its frequent tacit use to indicate runoff scarcity. However, there is no similar "apples and oranges" argument for the large gap between Q/P and AI responses, since Q/P is the quantity that AI classically predicts (Gentine et al., 2012; Budyko & Miller, 1974). Planned offline land-modeling work will test many of the above mechanisms.

For vegetation-related impacts (GPP and LAI), the substantial non-CO_2 portion of the simulated departure from the indices is most easily explained by the lengthening of mid-latitude growing seasons with global warming (e.g., Mankin et al., 2019), as stated in Section 3. Whether a longer growing season could overcome increased drought stress to cause greening in the real-world midlatitudes absent CO_2 effects is far from certain. However, observations to date (Zhu et al., 2016) show that greening has been much more prevalent than de-greening at all latitudes, including the mid-latitudes.

Finally, the almost total persistence of the gap between $\mathrm{SM_d}$ and $\mathrm{SM_s}$ responses when CO_2 effects are turned off strongly suggests that its main cause is the seasonal mechanism proposed by Berg et al. (2017), rather than plant savings of $\mathrm{SM_d}$ due to elevated CO_2. Similarly, the gap between EF and index responses is even stronger when CO_2 effects are off, so it must have a non-CO_2 cause, likely the basic thermodynamic EF increase with warming and/or the strong constraint of EF by radiation and P (Scheff, 2018).

5 Conclusion

A number of studies find that simple climatic dryness and drought indices, such as the Aridity Index (AI), Palmer Drought Severity Index (PDSI), and Standardized Precipitation-Evapotranspiration Index (SPEI), indicate much more widespread drying with climate change than implied by high-complexity models (and observations) of water resources and vegetation. Many of these studies ascribe this "index-impact gap" to the direct effects of CO_2 on plant physiology. To the contrary, here we show that much of this gap strongly persists even in specialized simulations (CMIP6 1pctCO2-rad; CMIP5 esmFdbk1) in which direct CO_2-plant effects are completely *turned off*, especially for impacts on water resources and mid-latitude vegetation. This strongly suggests key non-CO_2 cause(s) for the index-impact gap. Future work will test several candidate causes from the literature, using land-modeling experiments.

Acknowledgments

We acknowledge the World Climate Research Programme, which, through its Working Group on Coupled Modelling, coordinated and promoted CMIP6 and CMIP5. We thank the climate modeling groups for producing and making available their model output, the Earth System Grid Federation (ESGF) for archiving the data and providing access, and the multiple funding agencies who support CMIP and ESGF. All data is freely available at `https://esgf-node.llnl.gov/search/cmip6/` and `https://esgf-node.llnl.gov/search/cmip5/`. J. S. was supported by a UNC Charlotte Faculty Research Grant in 2019-20.

References

Allen, R. G., Pereira, L. S., Raes, D., & Smith, M. (1998). *Crop evapotranspiration: guidelines for computing crop water requirements* (Irrigation and Drainage Paper No. 56). Food and Agriculture Organization.

Allen, R. J., & Anderson, R. G. (2018). 21st century California drought risk linked to model fidelity of the El Niño teleconnection. *NPJ Climate and Atmospheric Science*, *1*, 21. doi: 10.1038/s41612-018-0032-x

AMS Council. (2013). *Drought: an information statement of the American Meteorological Society.* Retrieved from `https://www.ametsoc.org/ams/index.cfm/about-ams/ams-statements/statements-of-the-ams-in-force/drought/`

Arora, V. K., Boer, G. J., Friedlingstein, P., Eby, M., Jones, C. D., Christian, J. R., … Wu, T. (2013). Carbon-concentration and carbon-climate feedbacks in CMIP5 earth system models. *Journal of Climate*, *26*, 5289-5314. doi: 10.1175/JCLI-D-12-00494.1

Ault, T. R., Mankin, J. S., Cook, B. I., & Smerdon, J. E. (2016). Relative impacts of mitigation, temperature, and precipitation on 21st-century megadrought risk in the American Southwest. *Science Advances*, *2*, e1600873. doi: 10.1126/sciadv.1600873

Berg, A., Findell, K., Lintner, B., Giannini, A., Seneviratne, S. I., B. van den Hurk, … Milly, P. C. D. (2016). Land-atmosphere feedbacks amplify aridity increase over land under global warming. *Nature Climate Change*, *6*, 869-874. doi: 10.1038/nclimate3029

Berg, A., & Sheffield, J. (2018). Climate change and drought: the soil moisture perspective. *Current Climate Change Reports*, *4*, 180-191. doi: 10.1007/s40641-018-0095-0

Berg, A., Sheffield, J., & Milly, P. C. D. (2017). Divergent surface and total soil moisture projections under global warming. *Geophysical Research Letters*, *44*, 236-244. doi: 10.1002/2016GL071921

Bonan, G. (2015). *Ecological climatology: concepts and applications* (3rd ed.). Cambridge University Press. doi: 10.1017/CBO9781107339200

Boucher, O., Denvil, S., Caubel, A., & Foujols, M. A. (2018a). *IPSL IPSL-CM6A-LR model output prepared for CMIP6 C4MIP 1pctCO2-rad. Version 20180914.* Earth System Grid Federation. doi: 10.22033/ESGF/CMIP6.5051

Boucher, O., Denvil, S., Caubel, A., & Foujols, M. A. (2018b). *IPSL IPSL-CM6A-LR model output prepared for CMIP6 CMIP 1pctCO2. Version 20180727.* Earth System Grid Federation. doi: 10.22033/ESGF/CMIP6.5049

Brovkin, V., Wieners, K.-H., Giorgetta, M., Jungclaus, J., Reick, C., Esch, M., … Roeckner, E. (2019). *MPI-M MPI-ESM1.2-LR model output prepared for CMIP6 C4MIP 1pctCO2-rad. Version 20190710.* Earth System Grid Federation. doi: 10.22033/ESGF/CMIP6.6439

Brutsaert, W., & Parlange, M. B. (1998). Hydrologic cycle explains the evaporation paradox. *Nature*, *396*, 30.

Budyko, M. I., & Miller, D. H. (1974). *Climate and life.* Academic Press.

Byrne, M. P., & O'Gorman, P. A. (2016). Understanding decreases in land relative humidity with global warming: conceptual model and GCM simulations. *Journal of Climate*, *29*, 9045-9061. doi: 10.1175/JCLI-D-16-0351.1

Chou, C., Chiang, J. C. H., Lan, C.-W., Chung, C.-H., Liao, Y.-C., & Lee, C.-J. (2013). Increase in the range between wet and dry season precipitation. *Nature Geoscience*, *6*, 263-267. doi: 10.1038/NGEO1744

Cook, B. I., Ault, T. R., & Smerdon, J. E. (2015). Unprecedented 21st century drought risk in the American Southwest and Central Plains. *Science Advances*, *1*, e1400082. doi: 10.1126/sciadv.1400082

Cook, B. I., Smerdon, J. E., Seager, R., & Coats, S. (2014). Global warming and 21st century drying. *Climate Dynamics*, *43*, 2607-2627. doi: 10.1007/s00382-014-2075-y

Cook, E. R., Seager, R., Heim, R. R., Vose, R. S., Herweijer, C., & Woodhouse, C. (2009). Megadroughts in North America: placing IPCC projections of hydroclimatic change in a long-term palaeoclimate context. *Journal of Quaternary Science*, *25*, 48-61. doi: 10.1002/jqs.1303

Dai, A. (2013). Increasing drought under global warming in observations and models. *Nature Climate Change*, *3*, 52-58. doi: 10.1038/NCLIMATE1633

Dai, A., Zhao, T., & Chen, J. (2018). Climate change and drought: a precipitation and evaporation perspective. *Current Climate Change Reports*, *4*, 301-312. doi: 10.1007/s40641-018-0101-6

Eyring, V., Bony, S., Meehl, G. A., Senior, C. A., Stevens, B., Stouffer, R. J., &

Taylor, K. E. (2016). Overview of the Coupled Model Intercomparison Project Phase 6 (CMIP6) experimental design and organization. *Geoscientific Model Development*, *9*, 1937-1958. doi: 10.5194/gmd-9-1937-2016

Feng, S., & Fu, Q. (2013). Expansion of global drylands under a warming climate. *Atmospheric Chemistry and Physics*, *13*, 10081-10094. doi: 10.5194/acp-13-10081-2013

Fu, Q., & Feng, S. (2014). Responses of terrestrial aridity to global warming. *Journal of Geophysical Research*, *119*, 7863-7875. doi: 10.1002/2014JD021608

Fu, Q., Lin, L., Huang, J., Feng, S., & Gettelman, A. (2016). Changes in terrestrial aridity for the period 850-2080 from the Community Earth System Model. *Journal of Geophysical Research - Atmospheres*, *121*, 2857-2873. doi: 10.1002/2015JD024075

Gentine, P., D'Odorico, P., Lintner, B. R., Sivandran, G., & Salvucci, G. (2012). Interdependence of climate, soil, and vegetation as constrained by the Budyko curve. *Geophysical Research Letters*, *39*, L19404. doi: 10.1029/2012GL053492

Greve, P., Roderick, M. L., & Seneviratne, S. I. (2017). Simulated changes in aridity from the last glacial maximum to $4xCO_2$. *Environmental Research Letters*, *12*, 114021. doi: 10.1088/1748-9326/aa89a3

Greve, P., Roderick, M. L., Ukkola, A. M., & Wada, Y. (2019). The aridity index under global warming. *Environmental Research Letters*, *14*, 124006. doi: 10.1088/1748-9326/ab5046

Greve, P., & Seneviratne, S. I. (2015). Assessment of future changes in water availability and aridity. *Geophysical Research Letters*, *42*, 5493-5499. doi: 10.1002/2015GL064127

Hartmann, D. (2016). *Global physical climatology* (2nd ed.). Elsevier.

Huang, J., Yu, H., Guan, X., Wang, G., & Guo, R. (2015). Accelerated dryland expansion under climate change. *Nature Climate Change*, *6*, 166-171. doi: 10.1038/NCLIMATE2837

IPCC. (2013). Long-term climate change: projections, commitments and irreversibility. In T. Stocker et al. (Eds.), *Climate change 2013: the physical science basis. Contribution of Working Group I to the Fifth Assessment Report of the Intergovernmental Panel on Climate Change* (p. 1029-1136). Cambridge University Press.

Jones, C. D. (2019). *MOHC UKESM1.0-LL model output prepared for CMIP6 C4MIP 1pctCO2-rad. Version 20190904 for evspsbl, gpp, and lai; 20190723 for all others.* Earth System Grid Federation. doi: 10.22033/ESGF/CMIP6.5800

Jones, C. D., Arora, V., Friedlingstein, P., Bopp, L., Brovkin, V., Dunne, J., ... Zaehle, S. (2016). C4MIP - The Coupled Climate-Carbon Cycle Model Intercomparison Project: experimental protocol for CMIP6. *Geoscientific Model Development*, *9*, 2853-2880. doi: 10.5194/gmd-9-2853-2016

Krasting, J. P., Blanton, C., McHugh, C., Radhakrishnan, A., John, J. G., Rand, K., ... Zeng, Y. (2018). *NOAA-GFDL GFDL-ESM4 model output prepared for CMIP6 C4MIP 1pctCO2-rad. Version 20180701.* Earth System Grid Federation. doi: 10.22033/ESGF/CMIP6.8477

Krasting, J. P., John, J. G., Blanton, C., McHugh, C., Nikonov, S., Radhakrishnan, A., ... Zhao, M. (2018). *NOAA-GFDL GFDL-ESM4 model output prepared for CMIP6 CMIP 1pctCO2. Version 20180701.* Earth System Grid Federation. doi: 10.22033/ESGF/CMIP6.8473

Lehner, F., Coats, S., Stocker, T. F., Pendergrass, A. G., Sanderson, B. M., Raible, C. C., & Smerdon, J. E. (2017). Projected drought risk in 1.5°C and 2°C warmer climates. *Geophysical Research Letters*, *44*, 7419-7428. doi: 10.1002/2017GL074117

Lehner, F., Wood, A. W., Vano, J. A., Lawrence, D. M., Clark, M. P., & Mankin, J. S. (2019). The potential to reduce uncertainty in regional runoff projections from climate models. *Nature Climate Change*, *9*, 926-933. doi:

10.1038/s41558-019-0639-x

Lemordant, L., Gentine, P., Swann, A. S., Cook, B. I., & Scheff, J. (2018). Critical impact of vegetation physiology on the continental hydrologic cycle in response to increasing CO_2. *Proceedings of the National Academy of Sciences of the USA*, *115*, 4093-4098. doi: 10.1073/pnas.1720712115

Mankin, J. S., Seager, R., Smerdon, J. E., Cook, B. I., & Williams, A. P. (2019). Mid-latitude freshwater availability reduced by projected vegetation responses to climate change. *Nature Geoscience*, *12*, 983-988. doi: 10.1038/s41561-019-0480-x

Mankin, J. S., Seager, R., Smerdon, J. E., Cook, B. I., Williams, A. P., & Horton, R. M. (2018). Blue water trade-offs with vegetation in a CO_2-enriched climate. *Geophysical Research Letters*, *45*, 3115-3125. doi: 10.1002/2018GL077051

Massmann, A., Gentine, P., & Lin, C. (2019). When does vapor pressure deficit drive or reduce evapotranspiration? *Journal of Advances in Modeling Earth Systems*, *11*, 3305-3320. doi: 10.1029/2019MS001790

Middleton, N., & Thomas, D. S. G. (1997). *World atlas of desertification* (2nd ed.). Wiley.

Milly, P. C. D., & Dunne, K. A. (2016). Potential evapotranspiration and continental drying. *Nature Climate Change*, *6*, 946-949. doi: 10.1038/nclimate3046

Milly, P. C. D., & Dunne, K. A. (2017). A hydrologic drying bias in water-resource impact analyses of anthropogenic climate change. *Journal of the American Water Resources Association*, *53*, 822-838. doi: 10.1111/1752-1688.12538

Monteith, J. L. (1981). Evaporation and surface temperature. *Quarterly Journal of the Royal Meteorological Society*, *107*, 1-27.

NASA/GISS. (2019a). *NASA-GISS GISS-E2.1G model output prepared for CMIP6 C4MIP 1pctCO2-rad. Version 20190815.* Earth System Grid Federation. doi: 10.22033/ESGF/CMIP6.6958

NASA/GISS. (2019b). *NASA-GISS GISS-E2.1G model output prepared for CMIP6 CMIP 1pctCO2. Version 20190815.* Earth System Grid Federation. doi: 10.22033/ESGF/CMIP6.6950

Naumann, G., Alfieri, L., Wyser, K., Mentaschi, L., Betts, R. A., Carrao, H., ... Feyen, L. (2018). Global changes in drought conditions under different levels of warming. *Geophysical Research Letters*, *45*, 3285-3296. doi: 10.1002/2017GL076521

Novick, K. A., Ficklin, D. L., Stoy, P. C., Williams, C. A., Bohrer, G., Oishi, A. C., ... Phillips, R. P. (2016). The increasing importance of atmospheric demand for ecosystem water and carbon fluxes. *Nature Climate Change*, *6*, 1023-1027. doi: 10.1038/NCLIMATE3114

Palmer, W. C. (1965). *Meteorological drought* (Research Paper No. 45). U.S. Weather Bureau.

Park, C.-E., Jeong, S.-J., Joshi, M., Osborn, T. J., Ho, C.-H., Piao, S., ... Feng, S. (2018). Keeping global warming within 1.5 °C constrains emergence of aridification. *Nature Climate Change*, *8*, 70-74. doi: 10.1038/s41558-017-0034-4

Roderick, M. L., Greve, P., & Farquhar, G. D. (2015). On the assessment of aridity with changes in atmospheric CO2. *Water Resources Research*, *51*, 5450-5463. doi: 10.1002/2015WR017031

Scheff, J. (2018). Drought indices, drought impacts, CO_2, and warming: a historical and geologic perspective. *Current Climate Change Reports*, *4*, 202-209. doi: 10.1007/s40641-018-0094-1

Scheff, J., & Frierson, D. M. W. (2014). Scaling potential evapotranspiration with greenhouse warming. *Journal of Climate*, *27*, 1539-1558. doi: 10.1175/JCLI-D-13-00233.1

Scheff, J., & Frierson, D. M. W. (2015). Terrestrial aridity and its response to greenhouse warming across CMIP5 climate models. *Journal of Climate*, *28*, 5583-5600. doi: 10.1175/JCLI-D-14-00480.1

Scheff, J., Seager, R., Liu, H., & Coats, S. (2017). Are glacials dry? Consequences for paleoclimatology and for greenhouse warming. *Journal of Climate*, *30*, 6593-6609. doi: 10.1175/JCLI-D-16-0854.1

Schwinger, J., Tjiputra, J., Seland, Ø., Bentsen, M., Olivié, D. J. L., Toniazzo, T., … Schulz, M. (2020). *NCC NorESM2-LM model output prepared for CMIP6 C4MIP 1pctCO2-rad. Version 20200206.* Earth System Grid Federation. doi: 10.22033/ESGF/CMIP6.13726

Seager, R., Lis, N., Feldman, J., Ting, M., Williams, A., Nakamura, J., … Henderson, N. (2018). Whither the 100th meridian? The once and future physical and human geography of America's arid-humid divide. Part I: The story so far. *Earth Interactions*, *22*, 5. doi: 10.1175/EI-D-17-0011.1

Seferian, R. (2018a). *CNRM-CERFACS CNRM-ESM2-1 model output prepared for CMIP6 C4MIP 1pctCO2-rad. Version 20181113.* Earth System Grid Federation. doi: 10.22033/ESGF/CMIP6.3718

Seferian, R. (2018b). *CNRM-CERFACS CNRM-ESM2-1 model output prepared for CMIP6 CMIP 1pctCO2. Version 20181018.* Earth System Grid Federation. doi: 10.22033/ESGF/CMIP6.3714

Seland, Ø., Bentsen, M., Olivié, D. J. L., Toniazzo, T., Gjermundsen, A., Graff, L. S., … Schulz, M. (2019). *NCC NorESM2-LM model output prepared for CMIP6 CMIP 1pctCO2. Version 20191108 for sfcWind; 20190815 for all other Amon; 20190917 for Lmon.* Earth System Grid Federation. doi: 10.22033/ESGF/CMIP6.7802

Shao, P., Xubin Zeng, Sakaguchi, K., Monson, R. K., & Xiaodong Zeng. (2013). Terrestrial carbon cycle: climate relations in eight CMIP5 earth system models. *Journal of Climate*, *26*, 8744-8764. doi: 10.1175/JCLI-D-12-00831.1

Sherwood, S., & Fu, Q. (2014). A drier future? *Science*, *343*, 737-739. doi: 10.1126/science.1247620

Swann, A. L. S., Hoffman, F. M., Koven, C. D., & Randerson, J. T. (2016). Plant responses to increasing CO2 reduce estimates of climate impacts on drought severity. *Proceedings of the National Academy of Sciences of the USA*, *113*, 10019-10024. doi: 10.1073/pnas.1604581113

Swart, N. C., Cole, J. N., Kharin, V. V., Lazare, M., Scinocca, J. F., Gillett, N. P., … Sigmond, M. (2019a). *CCCma CanESM5 model output prepared for CMIP6 C4MIP 1pctCO2-rad. Version 20190429.* Earth System Grid Federation. doi: 10.22033/ESGF/CMIP6.3154

Swart, N. C., Cole, J. N., Kharin, V. V., Lazare, M., Scinocca, J. F., Gillett, N. P., … Sigmond, M. (2019b). *CCCma CanESM5 model output prepared for CMIP6 CMIP 1pctCO2. Version 20190429.* Earth System Grid Federation. doi: 10.22033/ESGF/CMIP6.3151

Tang, Y., Rumbold, S., Ellis, R., Kelley, D., Mulcahy, J., Sellar, A., … Jones, C. (2019). *MOHC UKESM1.0-LL model output prepared for CMIP6 CMIP 1pctCO2. Version 20190701 for evspsbl, gpp, and lai; 20190406 for all others.* Earth System Grid Federation. doi: 10.22033/ESGF/CMIP6.5792

Taylor, K. E., Stouffer, R. J., & Meehl, G. A. (2012). An overview of CMIP5 and the experiment design. *Bulletin of the American Meteorological Society*, *93*, 485-498. doi: 10.1175/BAMS-D-11-00094.1

Touma, D., Ashfaq, M., Nayak, M., Kao, S.-C., & Diffenbaugh, N. S. (2015). A multi-model and multi-index evaluation of drought characteristics in the 21st century. *Journal of Hydrology*, *526*, 196-207. doi: 10.1016/j.jhydrol.2014.12.011

Transeau, E. N. (1905). Forest centers of eastern America. *Amer. Naturalist*, *39*, 875-889.

Vicente-Serrano, S. M., Beguería, S., & López-Moreno, J. I. (2010). A multi-scalar drought index sensitive to global warming: the standardized precipitation evapotranspiration index. *Journal of Climate*, *23*, 1696-1718. doi:

10.1175/2009JCLI2909.1
Vicente-Serrano, S. M., McVicar, T. R., Miralles, D. G., Yang, Y., & Tomas-Burguera, M. (2019). Unraveling the influence of atmospheric evaporative demand on drought and its response to climate change. *WIREs Climate Change*, *11*, e632. doi: 10.1002/wcc.632
Wang, X., Jiang, D., & Lang, X. (2020). Future changes in Aridity Index at two and four degrees of global warming above preindustrial levels. *International Journal of Climatology*. doi: 10.1002/joc.6620
Wieners, K.-H., Giorgetta, M., Jungclaus, J., Reick, C., Esch, M., Bittner, M., ... Roeckner, E. (2019). *MPI-M MPI-ESM1.2-LR model output prepared for CMIP6 CMIP 1pctCO2. Version 20190710.* Earth System Grid Federation. doi: 10.22033/ESGF/CMIP6.6435
Wilhite, D. A., & Glantz, M. H. (1985). Understanding the drought phenomenon: the role of definitions. *Water International*, *10*, 111-120. doi: 10.1080/02508068508686328
Wu, T., Chu, M., Dong, M., Fang, Y., Jie, W., Li, J., ... Zhang, Y. (2018). *BCC BCC-CSM2MR model output prepared for CMIP6 CMIP 1pctCO2. Version 20181012 for Lmon and 20181015 for Amon.* Earth System Grid Federation. doi: 10.22033/ESGF/CMIP6.2833
Wu, T., Chu, M., Dong, M., Fang, Y., Jie, W., Li, J., ... Zhang, Y. (2019). *BCC BCC-CSM2MR model output prepared for CMIP6 C4MIP 1pctCO2-rad. Version 20190313 for Lmon and 20190321 for Amon.* Earth System Grid Federation. doi: 10.22033/ESGF/CMIP6.2836
Yang, Y., Roderick, M. L., Zhang, S., McVicar, T. R., & Donohue, R. J. (2019). Hydrologic implications of vegetation response to elevated CO_2 in climate projections. *Nature Climate Change*, *9*, 44-48. doi: 10.1038/s41558-018-0361-0
Yang, Y., Zhang, S., Roderick, M. L., McVicar, T. R., Yang, D., Liu, W., & Li, X. (2020). Comparing PDSI drought assessments using the traditional offline approach with direct climate model outputs. *Hydrology and Earth System Science*, *24*, 2921-2930. doi: 10.5194/hess-24-2921-2020
Yukimoto, S., Koshiro, T., Kawai, H., Oshima, N., Yoshida, K., Urakawa, S., ... Adachi, Y. (2020a). *MRI MRI-ESM2.0 model output prepared for CMIP6 C4MIP 1pctCO2-rad. Version 20191205 for Amon and 20200313 for Lmon.* Earth System Grid Federation. doi: 10.22033/ESGF/CMIP6.5358
Yukimoto, S., Koshiro, T., Kawai, H., Oshima, N., Yoshida, K., Urakawa, S., ... Adachi, Y. (2020b). *MRI MRI-ESM2.0 model output prepared for CMIP6 CMIP 1pctCO2. Version 20191205 for Amon and 20200313 for Lmon.* Earth System Grid Federation. doi: 10.22033/ESGF/CMIP6.5356
Zarch, M. A. A., Sivakumar, B., Malekinezhad, H., & Sharma, A. (2017). Future aridity under conditions of global climate change. *Journal of Hydrology*, *554*, 451-469. doi: 10.1016/j.jhydrol.2017.08.043
Zhao, T., & Dai, A. (2015). The magnitude and causes of global drought changes in the twenty-first century under a low-moderate emissions scenario. *Journal of Climate*, *28*, 4490-4512. doi: 10.1175/JCLI-D-14-00363.1
Zhao, T., & Dai, A. (2016). Uncertainties in historical changes and future projections of drought. Part II: model-simulated historical and future drought changes. *Climatic Change*, *144*, 535-548. doi: 10.1007/s10584-016-1742-x
Zhu, Z., Piao, S., Myneni, R. B., Huang, M., Zeng, Z., Canadell, J. G., ... Zeng, N. (2016). Greening of the Earth and its drivers. *Nature Climate Change*, *6*, 791-795. doi: 10.1038/NCLIMATE3004
Ziehn, T., Chamberlain, M., Lenton, A., Law, R., Bodman, R., Dix, M., ... Ridzwan, S. M. (2019a). *CSIRO ACCESS-ESM1.5 model output prepared for CMIP6 C4MIP 1pctCO2-rad. Version 20191118.* Earth System Grid Federation. doi: 10.22033/ESGF/CMIP6.4234
Ziehn, T., Chamberlain, M., Lenton, A., Law, R., Bodman, R., Dix, M., ... Druken,

K. (2019b). *CSIRO ACCESS-ESM1.5 model output prepared for CMIP6 CMIP 1pctCO2. Version 20191115.* Earth System Grid Federation. doi: 10.22033/ESGF/CMIP6.4231

Supporting Information for "CO_2-plant effects do not account for the gap between dryness indices and projected dryness impacts"

Jacob Scheff[1], Justin S. Mankin[2,4], Sloan Coats[3], and Haibo Liu[4]

[1]Dept. of Geography and Earth Sciences, University of North Carolina Charlotte

[2]Dept. of Geography and Dept. of Earth Sciences, Dartmouth College

[3]Dept. of Earth Sciences, University of Hawaii

[4]Lamont-Doherty Earth Observatory of Columbia University

Contents of this file

Introduction

Table S1 specifies the CMIP6 models used in the main text, including Figures 1-4. Table S2 specifies the CMIP5 models used in Figures S3-S6. Figures S1-S2 reproduce Figures 1-2 from the main text, but with each model's changes normalized by that model's year-to-year standard deviation. Figures S3-S6 reproduce Figures 1-4 from the main text, but for CMIP5.

References

Boucher, O., Denvil, S., Caubel, A., & Foujols, M. A. (2018a). *IPSL IPSL-CM6A-LR model output prepared for CMIP6 C4MIP 1pctCO2-rad. Version 20180914.* Earth System Grid Federation. doi: 10.22033/ESGF/CMIP6.5051

Boucher, O., Denvil, S., Caubel, A., & Foujols, M. A. (2018b). *IPSL IPSL-CM6A-LR model output prepared for CMIP6 CMIP 1pctCO2. Version 20180727.* Earth System Grid Federation. doi: 10.22033/ESGF/CMIP6.5049

Brovkin, V., Wieners, K.-H., Giorgetta, M., Jungclaus, J., Reick, C., Esch, M., ... Roeckner, E. (2019). *MPI-M MPI-ESM1.2-LR model output prepared for CMIP6 C4MIP 1pctCO2-rad. Version 20190710.* Earth System Grid Federation. doi: 10.22033/ESGF/CMIP6.6439

Jones, C. D. (2019). *MOHC UKESM1.0-LL model output prepared for CMIP6 C4MIP 1pctCO2-rad. Version 20190904 for evspsbl, gpp, and lai; 20190723 for all others.* Earth System Grid Federation. doi: 10.22033/ESGF/CMIP6.5800

Krasting, J. P., Blanton, C., McHugh, C., Radhakrishnan, A., John, J. G., Rand, K., ... Zeng, Y. (2018). *NOAA-GFDL GFDL-ESM4 model output prepared for CMIP6 C4MIP 1pctCO2-rad. Version 20180701.* Earth System Grid Federation. doi: 10.22033/ESGF/CMIP6.8477

Krasting, J. P., John, J. G., Blanton, C., McHugh, C., Nikonov, S., Radhakrishnan, A., ... Zhao, M. (2018). *NOAA-GFDL GFDL-ESM4 model output prepared for CMIP6 CMIP 1pctCO2. Version 20180701.* Earth System Grid Federation. doi: 10.22033/ESGF/CMIP6.8473

NASA/GISS. (2019a). *NASA-GISS GISS-E2.1G model output prepared for CMIP6 C4MIP 1pctCO2-rad. Version 20190815.* Earth System Grid Federation. doi: 10.22033/ESGF/CMIP6.6958

NASA/GISS. (2019b). *NASA-GISS GISS-E2.1G model output prepared for CMIP6 CMIP 1pctCO2. Version 20190815.* Earth System Grid Federation. doi: 10.22033/ESGF/CMIP6.6950

Schwinger, J., Tjiputra, J., Seland, Ø., Bentsen, M., Olivié, D. J. L., Toniazzo, T., ... Schulz, M. (2020). *NCC NorESM2-LM model output prepared for CMIP6 C4MIP 1pctCO2-rad. Version 20200206.* Earth System Grid Federation. doi: 10.22033/ESGF/CMIP6.13726

Seferian, R. (2018a). *CNRM-CERFACS CNRM-ESM2-1 model output prepared for CMIP6 C4MIP 1pctCO2-rad. Version 20181113.* Earth System Grid Federation. doi: 10.22033/ESGF/CMIP6.3718

Seferian, R. (2018b). *CNRM-CERFACS CNRM-ESM2-1 model output prepared for CMIP6 CMIP 1pctCO2. Version 20181018.* Earth System Grid Federation. doi: 10.22033/ESGF/CMIP6.3714

Seland, Ø., Bentsen, M., Olivié, D. J. L., Toniazzo, T., Gjermundsen, A., Graff, L. S., ... Schulz, M. (2019). *NCC NorESM2-LM model output prepared for CMIP6 CMIP 1pctCO2. Version 20191108 for sfcWind; 20190815 for all other Amon; 20190917 for Lmon.* Earth System Grid Federation. doi: 10.22033/ESGF/CMIP6.7802

Swart, N. C., Cole, J. N., Kharin, V. V., Lazare, M., Scinocca, J. F., Gillett, N. P., ... Sigmond, M. (2019a). *CCCma CanESM5 model output prepared for CMIP6 C4MIP*

1pctCO2-rad. Version 20190429. Earth System Grid Federation. doi: 10.22033/ESGF/CMIP6.3154

Swart, N. C., Cole, J. N., Kharin, V. V., Lazare, M., Scinocca, J. F., Gillett, N. P., ... Sigmond, M. (2019b). *CCCma CanESM5 model output prepared for CMIP6 CMIP 1pctCO2. Version 20190429.* Earth System Grid Federation. doi: 10.22033/ESGF/CMIP6.3151

Tang, Y., Rumbold, S., Ellis, R., Kelley, D., Mulcahy, J., Sellar, A., ... Jones, C. (2019). *MOHC UKESM1.0-LL model output prepared for CMIP6 CMIP 1pctCO2. Version 20190701 for evspsbl, gpp, and lai; 20190406 for all others.* Earth System Grid Federation. doi: 10.22033/ESGF/CMIP6.5792

Wieners, K.-H., Giorgetta, M., Jungclaus, J., Reick, C., Esch, M., Bittner, M., ... Roeckner, E. (2019). *MPI-M MPI-ESM1.2-LR model output prepared for CMIP6 CMIP 1pctCO2. Version 20190710.* Earth System Grid Federation. doi: 10.22033/ESGF/CMIP6.6435

Wu, T., Chu, M., Dong, M., Fang, Y., Jie, W., Li, J., ... Zhang, Y. (2018). *BCC BCC-CSM2MR model output prepared for CMIP6 CMIP 1pctCO2. Version 20181012 for Lmon and 20181015 for Amon.* Earth System Grid Federation. doi: 10.22033/ESGF/CMIP6.2833

Wu, T., Chu, M., Dong, M., Fang, Y., Jie, W., Li, J., ... Zhang, Y. (2019). *BCC BCC-CSM2MR model output prepared for CMIP6 C4MIP 1pctCO2-rad. Version 20190313 for Lmon and 20190321 for Amon.* Earth System Grid Federation. doi: 10.22033/ESGF/CMIP6.2836

Yukimoto, S., Koshiro, T., Kawai, H., Oshima, N., Yoshida, K., Urakawa, S., ... Adachi, Y. (2020a). *MRI MRI-ESM2.0 model output prepared for CMIP6 C4MIP 1pctCO2-rad. Version 20191205 for Amon and 20200313 for Lmon.* Earth System Grid Federation. doi: 10.22033/ESGF/CMIP6.5358

Yukimoto, S., Koshiro, T., Kawai, H., Oshima, N., Yoshida, K., Urakawa, S., ... Adachi, Y. (2020b). *MRI MRI-ESM2.0 model output prepared for CMIP6 CMIP 1pctCO2. Version 20191205 for Amon and 20200313 for Lmon.* Earth System Grid Federation. doi: 10.22033/ESGF/CMIP6.5356

Ziehn, T., Chamberlain, M., Lenton, A., Law, R., Bodman, R., Dix, M., ... Ridzwan, S. M. (2019a). *CSIRO ACCESS-ESM1.5 model output prepared for CMIP6 C4MIP 1pctCO2-rad. Version 20191118.* Earth System Grid Federation. doi: 10.22033/ESGF/CMIP6.4234

Ziehn, T., Chamberlain, M., Lenton, A., Law, R., Bodman, R., Dix, M., ... Druken, K. (2019b). *CSIRO ACCESS-ESM1.5 model output prepared for CMIP6 CMIP 1pctCO2. Version 20191115.* Earth System Grid Federation. doi: 10.22033/ESGF/CMIP6.4231

Table S1. CMIP6 climate models analyzed in this study

Model name	Institution	Data citations
ACCESS-ESM1.5	CSIRO	Ziehn et al. (2019a, 2019b)
BCC-CSM2MR	BCC	Wu et al. (2018, 2019)
CanESM5	CCCma	Swart et al. (2019a, 2019b)
CNRM-ESM2-1[a]	CNRM-CERFACS	Seferian (2018a, 2018b)
GFDL-ESM4[a]	NOAA-GFDL	Krasting, John, et al. (2018); Krasting, Blanton, et al. (2018)
GISS-E2.1G[b]	NASA-GISS	NASA/GISS (2019a, 2019b)
IPSL-CM6A-LR	IPSL	Boucher, Denvil, Caubel, and Foujols (2018a, 2018b)
MPI-ESM1.2-LR	MPI-M	Wieners et al. (2019); Brovkin et al. (2019)
MRI-ESM2.0[c]	MRI	Yukimoto et al. (2020a, 2020b)
NorESM2-LM[d]	NCC	Seland et al. (2019); Schwinger et al. (2020)
UKESM1.0-LL	MOHC	Tang et al. (2019); Jones (2019)

[a] SM_d is not available.
[b] We use r101 for 1pctCO2, since it is the most up-to-date and matches 1pctCO2-rad.
[c] We use i2, since i1 lacks carbon cycle variables (S. Yukimoto, pers. comm.)
[d] Base period is years 2-31, since part of year 1 is missing for some variables.

Table S2. CMIP5 climate models used for Figs. S3-S6

Model name	Institution
BCC-CSM1.1	Beijing Climate Center, China Meteorological Administration
CanESM2	Canadian Centre for Climate Modelling and Analysis
CESM1(BGC)	Community Earth System Model Contributors
GFDL-ESM2M	NOAA Geophysical Fluid Dynamics Laboratory
HadGEM2-ES	Met Office Hadley Centre
IPSL-CM5A-LR[a]	Institut Pierre-Simon Laplace
IPSL-CM5A-MR[a]	
MPI-ESM-LR[a,b]	Max Planck Institute for Meteorology
NorESM1-ME	Norwegian Climate Centre

[a] SM_d is not available.
[b] SM_s is not available.

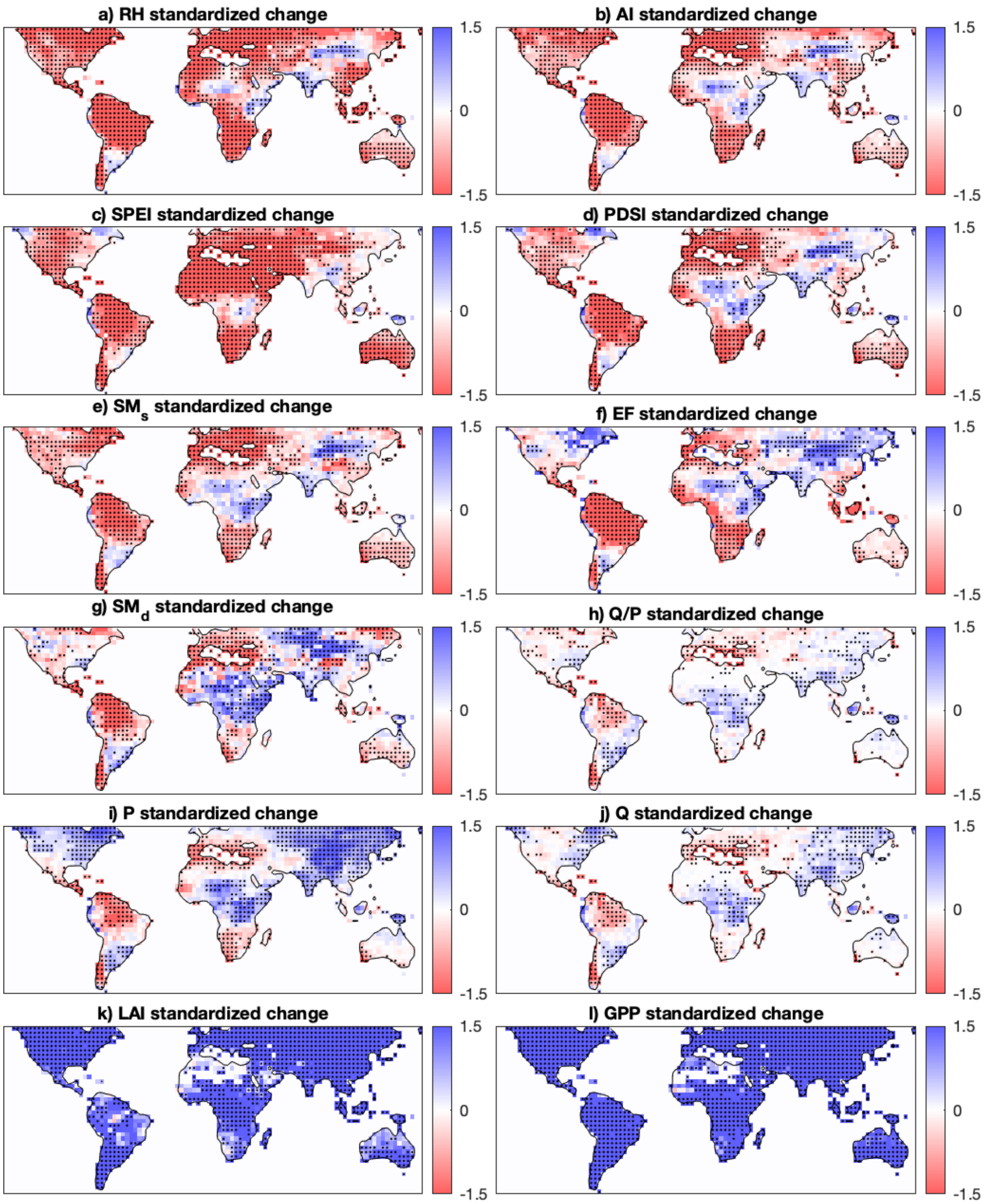

Figure S1. As Fig. 1 of the main text, but each model's response is normalized by that model's interannual standard deviation before the multi-model median is taken. Annual Q each year is defined as annual P minus annual ET; this is not strictly correct (due to storage) but should capture the magnitude of interannual standard deviation of Q. Annual EF and Q/P are each defined as the ratio of the yearly values of their numerator and denominator. "Interannual variability of AI" is represented by interannual standard deviation of P over climatological E_0.

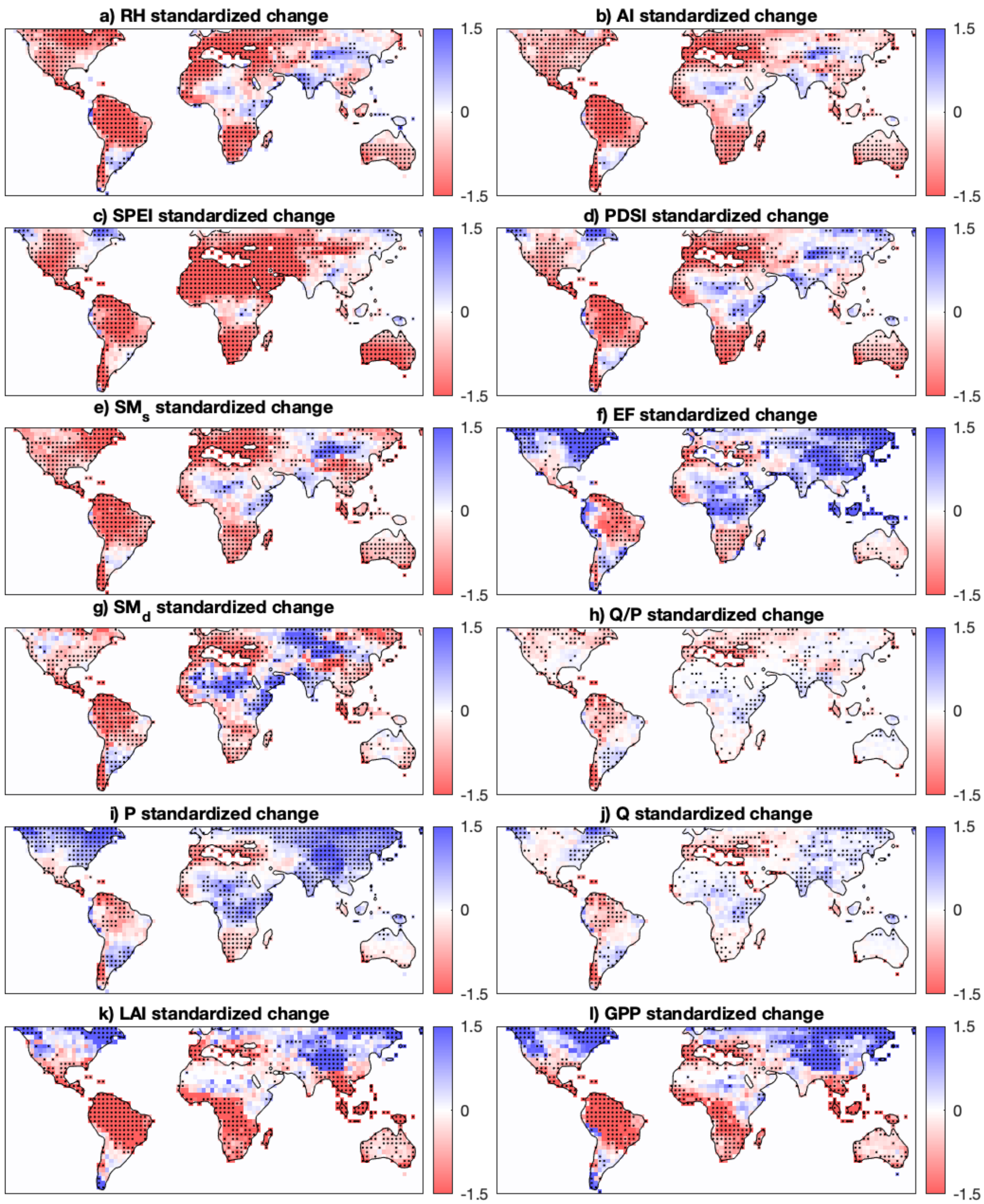

Figure S2. As Fig. S1, but for Fig. 2 of the main text (1pctCO2-rad experiment.)

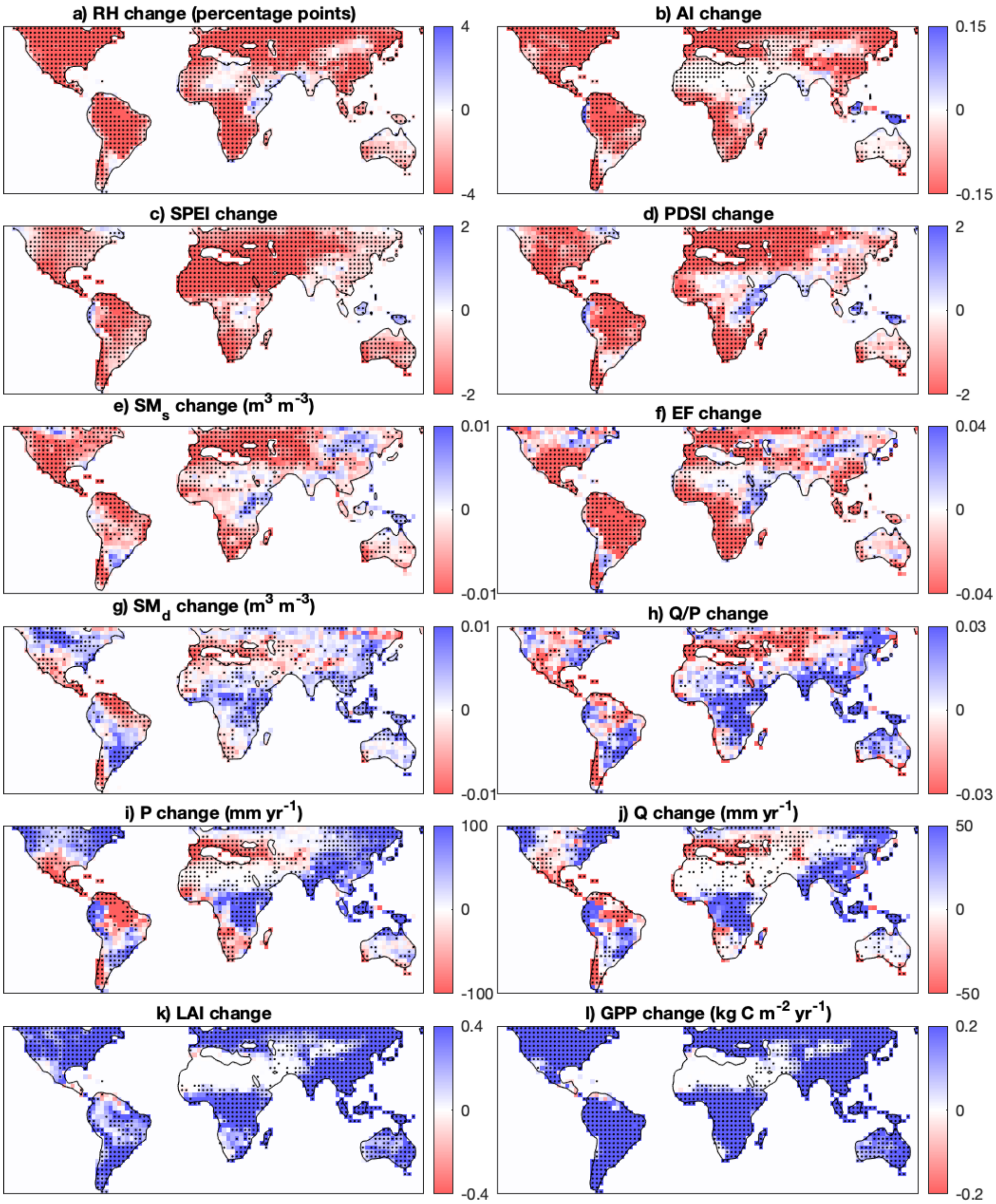

Figure S3. As Fig. 1 of the main text, but for the CMIP5 models in Table S2.

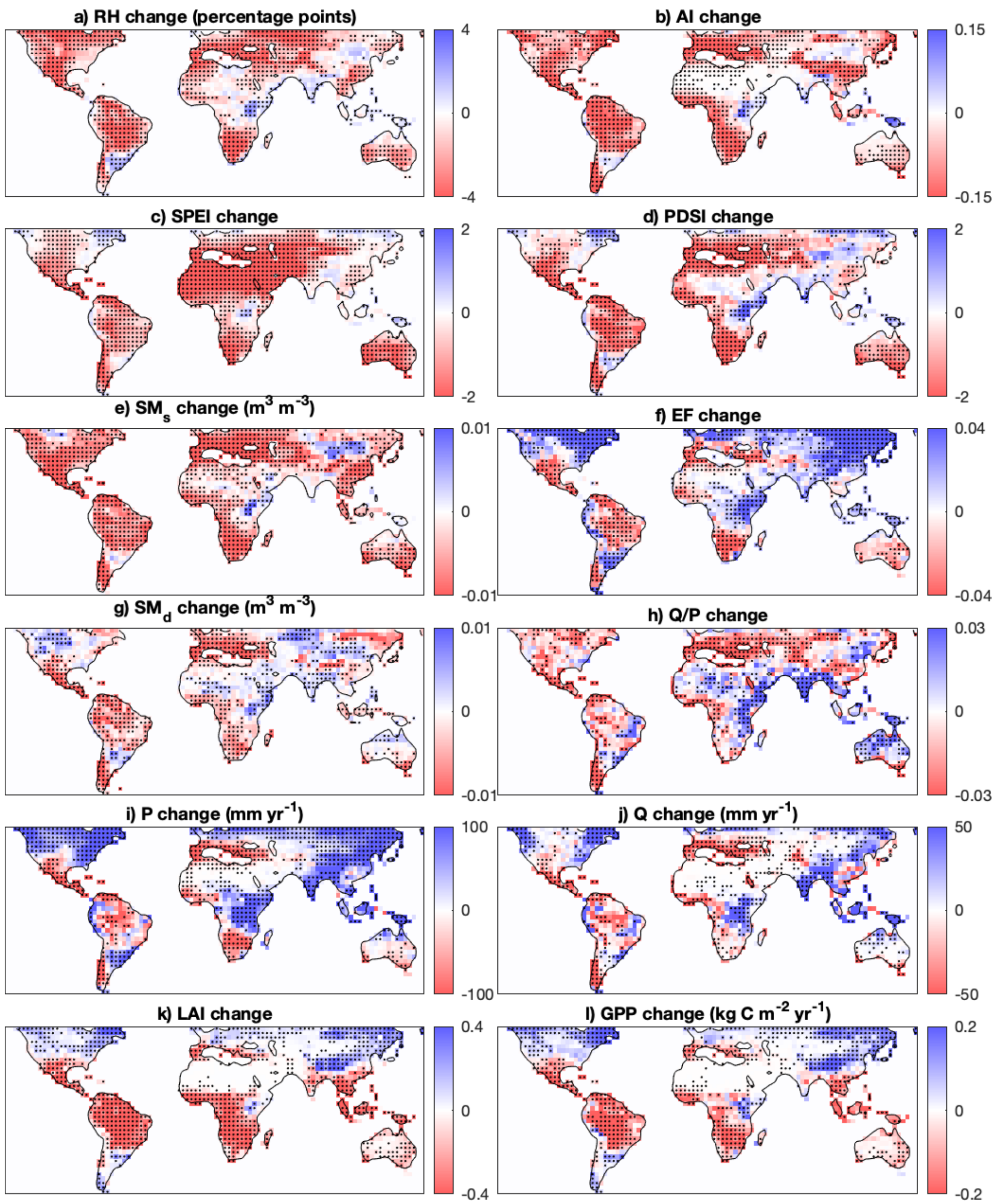

Figure S4. As Fig. 2 of the main text, but for the CMIP5 models in Table S2, using the esmFdbk1 experiment (identical to 1pctCO2-rad, except for the name.)

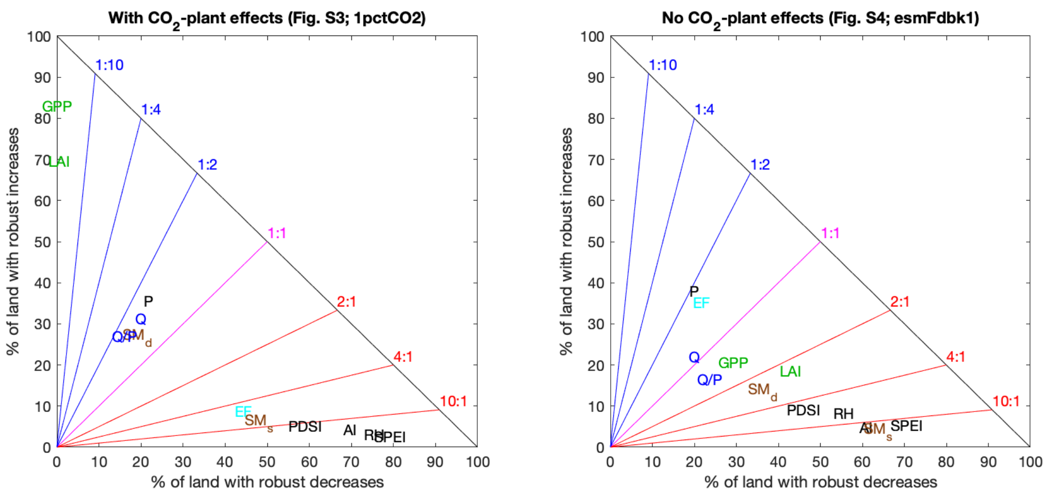

Figure S5. As Fig. 3 of the main text, but for Figs. S3 and S4.

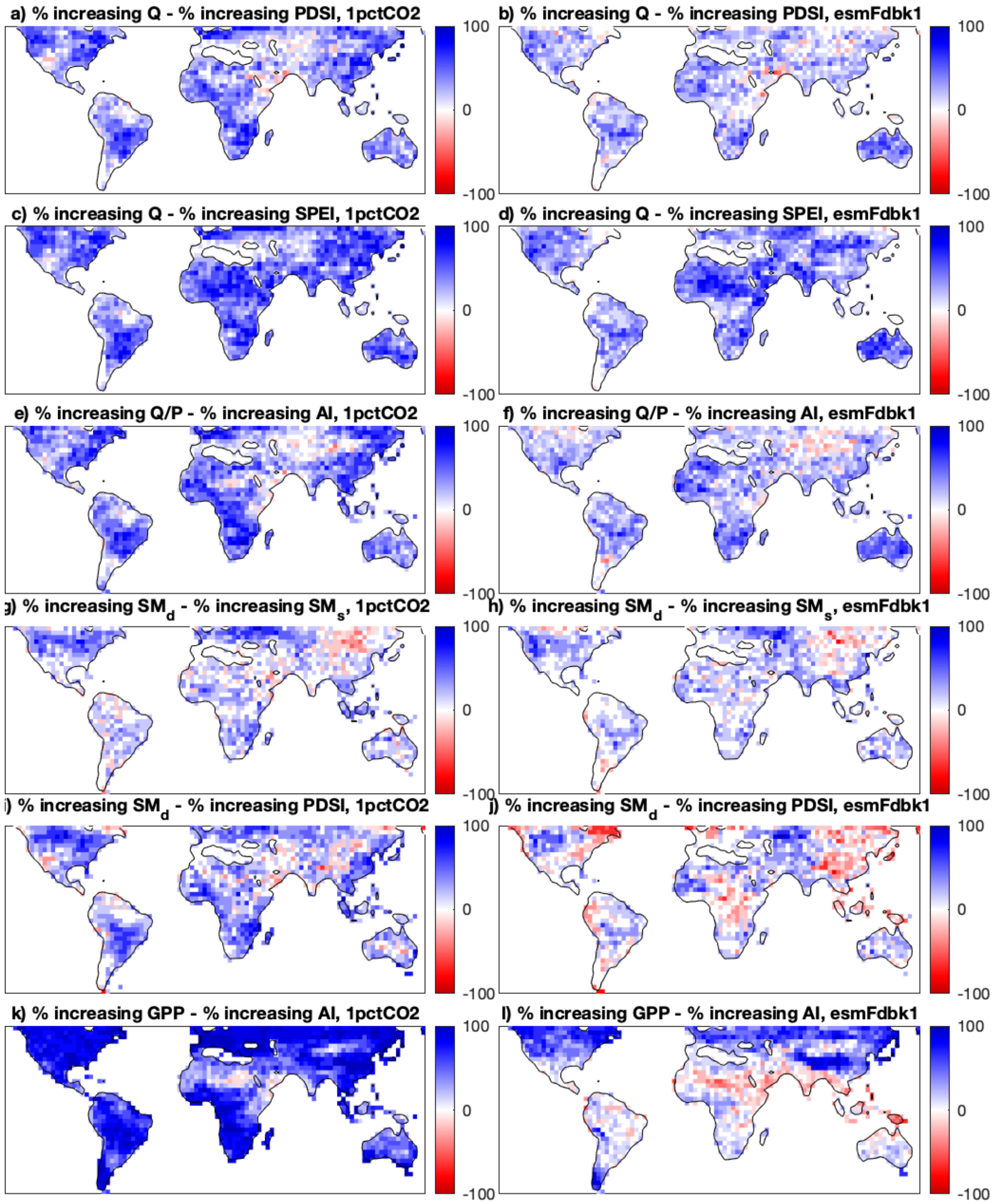

Figure S6. As Fig. 4 of the main text, but for the CMIP5 models in Table S2.